Journal Name

ARTICLE TYPE

Cite this: DOI: 10.1039/xxxxxxxxxx

Supporting Information: Fibrillation-prone conformations of the amyloid-β-42 peptide at the gold/water interface

Luca Bellucci,*[a] Giovanni Bussi,[b] Rosa Di Felice,[c] Stefano Corni*[a]

1 Methods and computational details

All simulations were performed with GROMACS[1] (v4.5.3) togheter with PLUMED[2] (v1.3) plug-in. All simulations were performed in explicit solvent using TIP3P[3] water model. The Aβ42 was treated with the OPLS-AA[4] FF, while interaction between the peptide and gold surface was treated with the GolP FF[5]. GolP extends the OPLS-AA parameters[4] by interactions of amino acid building blocks with Au(111) and includes a term that describes metal polarizability[6]. GolP yielded impressive results in previous applications[7–12] and it also has a CHARMM version[13]. The model to treat the surface polarizability was recently extended to other materials, specifically graphene[14]. It has been proved that MD simulations employing the OPLS-AA force field to treat Aβ can reproduce experimental results[15] and they have been proficiently used in recent computational works[16–18].

All the simulations were performed using periodic boundary conditions (PBC) and an integration time step of 2 fs. The long-range part of the electrostatic potential was treated with the Particle-Mesh-Ewald (PME) protocol[19] with a grid mesh not exceeding 1 step for 0.1 nm. The distance cut-off for non-bonded interactions was set to 1.05 nm and a switch function was applied to smooth interactions between 0.9 and 1.05 nm. All bonds were treated as holonomic constraints using the LINCS algorithm[20]. The temperature was maintained constant using the stochastic thermostat[21] with a coupling constant of 0.1 ps^{-1}. The pressure in the NPT ensemble was regulated using the Parrinello-Rahman barostat[22].

2 Sequential multi-step simulation protocol

Here we describe the four sequential steps to go from a representative ensemble of Aβ42 in solution to the intensive sampling of Aβ42 at the gold/water interface. Aβ42 does not attain a specific three-dimensional structure, but it consists of a broad and fluctuating ensemble of conformations in equilibrium with each other. Moreover, the adsorption of Aβ42 involves many dynamical stages, from the initial recognition of the molecules by the surface to the conformational rearrangements of the adsorbed molecules to reach equilibrium. To study how NPs or surfaces could affect the behavior of Aβ42, it was necessary to (i) prepare the system starting from database knowledge; (ii) supply a representative ensemble of the conformational states of the Aβ42 in solution; (iii) adsorb Aβ42 onto the gold surface; and, finally, (iv) perform an intensive sampling of the adsorbed Aβ42 conformers on the gold surface.

2.1 Preparation of the peptide: Aβ42 from the membrane environment to the early stage in solution

The initial structure for Aβ42 was selected from the NMR structure resolved in an aqueous/hexafluoroisopropanol mixture, which reproduces the membrane environment[23] (PDB ID 1IYT, model 1). This peptide was placed in the center of a cubic box of 7.2 nm side and solvated with 12191 water molecules. Three Na^+ counter ions were added to neutralize the total charge of the system.

The system was minimized with 1300 conjugate gradient steps. A preliminary MD equilibration of 2 ns was performed in the NVT ensemble at 350 K. The system was simulated in the NPT ensemble (1 atm, 350 K) for 20 ns to disengage from the NMR struc-

[a] Center S3, CNR Institute of Nanoscience, via Campi 213/A, 41125 Modena, Italy E-Mail: stefano.corni@nano.cnr.it; luca.bellucci@nano.cnr.it
[b] SISSA- Scuola Internazionale Superiore di Studi Avanzati, via Bonomea 265, 34136 Trieste, Italy
[c] Department of Physics and Astronomy, University of Southern California, Los Angeles, CA 90089, USA

†Electronic Supplementary Information (ESI) available: methods and computational details, distance distribution function, of Aβ42 in water, Computed chemical shifts and J-couplings, contact fraction and pathway and rotations of the center of mass (COM) and adsorption percentage nad RMSD of Aβ42 and radius of gyration during the adsorption process, chemical shift evaluate ad to gold surface, acylindricity and asphericity, percentage of secondary structures, distribution of the radius of gyration over representative structures obtained from clustering, distribution of the RMSD values of Aβ with respect to experimental fiber structures. See DOI

ture. Then the system was subjected to a second equilibration in the NPT ensemble at 300 K for 20 ns. Finally, a MD simulation in the NVT ensemble (300 K) was carried out for 20 ns. During these MD simulations alpha helix content of the peptide, which is characteristic of the membrane environment (Fig. S1 A), changed towards a collapsed conformation, which is instead more stable in aqueous solution (Fig. S1 B). The final coordinates obtained from this set of simulations was used to set up the 64 replicas for the T-REMD simulation.

2.2 Sampling the conformational ensemble of Aβ42 in water by T-REMD [ABWT-TREMD]

We employed the temperature replica-exchange molecular dynamics (T-REMD) technique[24] to generate a representative ensemble of the conformational states of the peptide in water. T-REMD consisted of 64 replicas spanning a temperature range from 300 to 450 K. Intervals were evaluated following a scheme reported elsewhere[25]. Exchange between replicas was performed every 0.2 ps. The average acceptance ratio among the replicas at end of the T-REMD simulation was about 20%. Each replica was simulated in the NVT ensemble[21] for 0.34 μs, totaling a cumulative time of 22 μs. To take into account the possibility of inter-conversion among different conformational states that could proceed through extended intermediates, the T-REMD simulation was carried out using a cubic box with a side length of 7.2 nm. This size is adequate to sample elongated conformers (Fig. S4).

2.3 Early stage of adsorption of Aβ42 on Au(111) in water [ABAU-MD]

We selected 128 conformations of Aβ42 from the last 128 ns of replica 0 (the replica at 300 K) of the T-REMD simulation. One conformer was selected at each ns and placed in the middle of a box with size $9.1\times8.8\times8.5$ nm^3 containing a gold slab (5 layers, 1 nm thick) and 19661 water molecules. These 128 systems were subjected to unconstrained MD for 20 ns at 300K in the NVT ensemble, to trace the adsorption dynamics of Aβ42 onto the gold surface. During the initial stages of the MD simulations, the distances between the gold and protein atoms were greater than 2 nm, and thus, the interactions between the peptide and the gold surface were negligible (Fig. S2). It is worth noting that the 128 initial conformers reflected all the features of the "structural categories" that Aβ42 can populate in solution (Fig. S3).

2.4 Aβ42 at the gold/water interface by HT-REMD [ABAU-HTREMD]

The Hamiltonian-Temperature-Replica-Exchange-MD (HT-REMD) technique was used to ensure an adequate sampling of the peptide-covered substrate[26]. HT-REMD is a variant of T-REMD that allows interactions between different portions of the system to be scaled, in order to raise the probability of overcoming the barriers between states of the system. In HT-REMD, N copies of the system (replicas) run concurrently at different temperatures and with scaled Hamiltonians between different portions of the system (i.e., scaling the interactions between gold and protein). On the one hand, scaling the specific gold-protein potential in the modified-Hamiltonian replicas, it is possible to decrease the high energy barriers due to the interactions between the surface and the peptide. On the other hand, with the use of high temperatures it is possible to accelerate the crossing of the energy barriers of the whole system. Exchanges of the configurations of neighboring replicas are attempted at fixed intervals, and are accepted or rejected by means of a Metropolis test so as to ensure the correct thermodynamics ensemble. The HT-REMD protocol, therefore, represents a robust method to sample heterogeneous systems where the interactions among the various species can be very different in intensity.

HT-REMD was performed using 128 replicas. The initial conformations for the the 128 replicas were taken from ABAU-MD: the final structure from each one of the previous MD simulations was used to set up a replica. The temperatures of the replicas were between 300 and 450 K, whereas the gold/protein interactions were scaled starting from replica 20 (i.e. at 320 K). The scaling factor spanned between 1 and 0.6. Each replica lasted for 0.15 μs; the cumulative time of the HT-REMD simulation was 20 μs. Exchange between replicas was performed every 0.2 ps. The average acceptance ratio among the replicas at end of the HT-REMD simulation was about 40%.

3 Analysis of the results

For comparison between ABWT-TREMD and ABAU-HTREMD, we considered the last 0.1 μs of the first 20 replicas, (i.e., the non-scaled Hamiltonian replicas) of the HT-REMD and the last 0.2 μs of the first 10 replicas of the T-REMD, taking into account 1 conformation every 10 ps. The analysis was carried out in a series of conformations with a cumulative time of 4 μs, i.e, 2 μs for each system.

Analysis, where not mentioned, was performed with VMD[27](v1.9.2), GROMACS tools and PLUMED. The chemical shifts for the Cα atoms, which usually are the most significant indicators of protein secondary structure, were calculated using the SPARTA+ program[28]. The homonuclear HN-HA coupling constants were estimated evaluating the Karplus equation[29] using the coefficients reported elsewhere[18] (A=6.88, B -6.50, C=-3.53). Error analysis for the estimated J coupling constants was performed using the block average method[30]. The structural similarity was evaluated by the root mean square deviation (RMSD): if not specified, RMSD was evaluated for C$_\alpha$ atoms. Cluster analysis was performed using the "gromos" algorithm[31] available with the GROMACS tools, g_cluster: only the C$_\alpha$ atoms were included in the

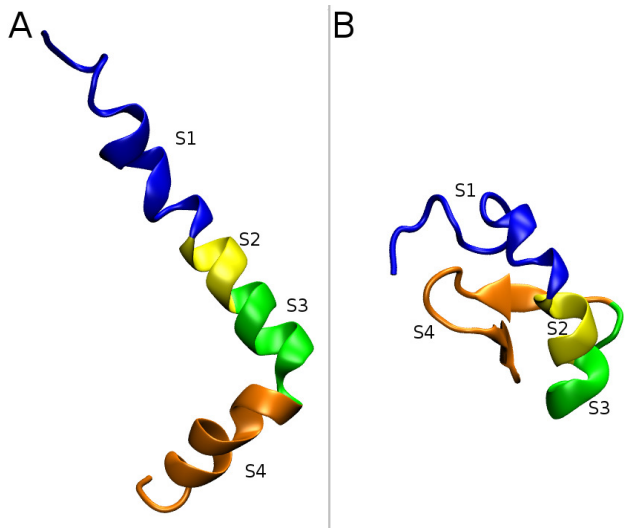

Fig. S1 Aβ42 in membrane environment and in solution. (A) The experimental NMR Aβ42 structure in the membrane environment (PDB ID 1YIT) shows a high α-helix content. Aβ42 is composed of 4 segments that differ from each other for their physical properties: the first segment (S1, blue, 1Asp-2Ala-3Glu-4Phe-5Arg-6His-7Asp-8Ser-9Gly-10Tyr-11Glu-12Val-13His-14His-15Gln-16Lys) is defined by residues 1-16 and has mainly hydrophilic properties; the segment 17-21 (S2, yellow,-17Leu-18Val-19Phe-20Phe-21Ala) is composed by hydrophobic and aromatic residues and is known as the "Aβ42 hydrophobic core"; the segment 22-29 (S3, green, -22Glu-23Asp-24Val-25Gly-26Ser-27Asn-28Lys-29Gly) in fibrils adopts a β turn shape; and finally the C-terminal tail 30-42 (S4, orange,-30Ala-31Ile-32Ile-33Gly-34Leu-35Met-36Val-37Gly-38Gly-39Val-40Val-41Ile-42Ala) is hydrophobic. (B) Final structure of Aβ42 from the preparatory MD trajectory in solution: the peptide collapses to a more compact shape. The C-terminal tail (S4) shows a high propensity to form a β-sheet. The core of the peptide remains in the α-helix conformation, whereas the N-terminal tail is mainly unstructured.

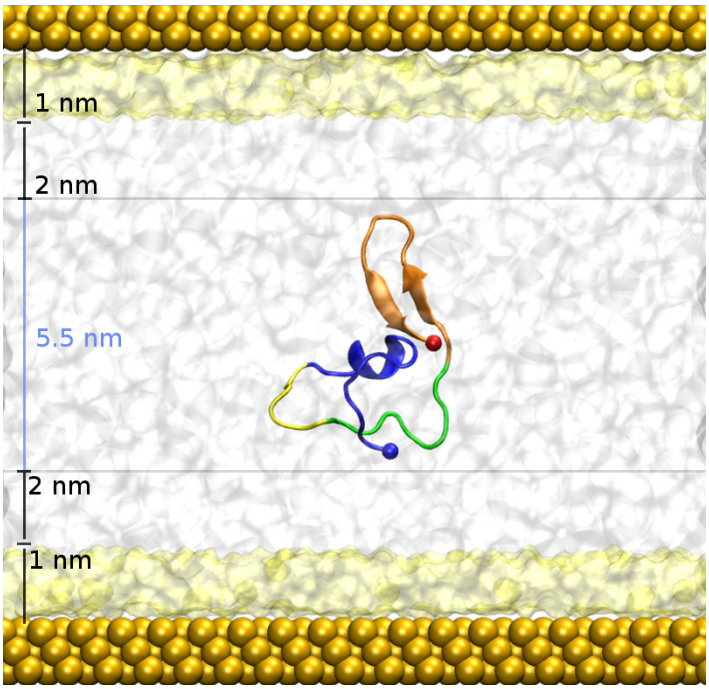

Fig. S2 Simulation Box. The system is composed of water, Aβ42 and five gold layers, specifically Au(111). Gold atoms are shown as yellow spheres. Water molecules are shown as a transparent material: those within 10 Å from the gold surface are yellow, bulk water is light gray. The C-terminal and N-terminal C_α atoms are shown in red and blue, respectively.

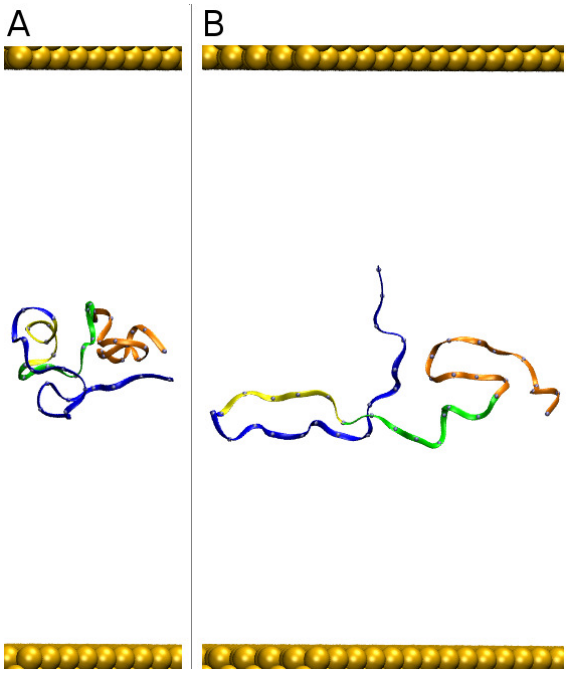

Fig. S3 . **Aβ42 structures used as starting points for the relaxation of the Aβ42 onto the gold surface.** Examples of two of the 128 Aβ42 conformers extracted from ABWT-TREMD and used as starting points to study the dynamics of the adsorption process. The yellow spheres represent the atoms of the two equivalent gold surfaces. Water molecules are not shown. A. A globular conformer. B. The most extended conformer among the selected structures: the maximum intramolecular distances between the C_α atoms of this structure is $r_{max}^{C_\alpha A - C_\alpha A}$=4.3 nm.

clustering procedure, using a C_α-RMSD cut-off of 0.28 nm. The secondary structure content was analyzed with the DSSP program[32].

References

1 B. Hess, C. Kutzner, D. Van Der Spoel and E. Lindahl, *J. Chem. Theory. Comput.*, 2008, **4**, 435–447.

2 M. Bonomi, D. Branduardi, G. Bussi, C. Camilloni, D. Provasi, P. Raiteri, D. Donadio, F. Marinelli, F. Pietrucci, R. Broglia and M. Parrinello, *Comput. Phys. Commun.*, 2009, **180**, 1961–1972.

3 W. L. Jorgensen, J. Chandrasekhar, J. D. Madura, R. W. Impey and M. L. Klein, *J. Chem. Phys.*, 1983, **79**, 926–935.

4 W. L. Jorgensen, D. S. Maxwell and J. Tirado-Rives, *J. Am. Chem. Soc.*, 1996, **118**, 11225–11236.

5 F. Iori, R. Di Felice, E. Molinari and S. Corni, *J. Comp. Chem.*, 2009, **30**, 1465–1476.

6 F. Iori and S. Corni, *J. Comput. Chem.*, 2008, **29**, 1656–1666.

7 M. Hoefling, F. Iori, S. Corni and K.-E. Gottschalk, *Langmuir*, 2010, **26**, 8347–8351.

8 R. Di Felice and S. Corni, *J. Phys. Chem. Lett.*, 2011, **2**, 1510–1519.

9 L. Bellucci and S. Corni, *J. Phys. Chem. C*, 2014, **118**, 11357–11364.

10 L. Zanetti-Polzi, I. Daidone, C. A. Bortolotti and S. Corni, *J. Am. Chem. Soc.*, 2014, **136**, 12929–12937.

11 G. Brancolini, D. Toroz and S. Corni, *Nanoscale*, 2014, **6**, 7903–7911.

12 S. Corni, M. Hnilova, C. Tamerler and M. Sarikaya, *J. Phys. Chem. C*, 2013, **117**, 16990–17003.

13 L. B. Wright, P. M. Rodger, S. Corni and T. R. Walsh, *J. Chem. Theory. Comput.*, 2013, **9**, 1616–1630.

14 Z. E. Hughes, S. M. Tomásio and T. R. Walsh, *Nanoscale*, 2014, **6**, 5438–5448.

15 S. R. Gerben, J. A. Lemkul, A. M. Brown and D. R. Bevan, *J. Biomol. Struct. Dyn.*, 2014, **32**, 1817–1832.

16 N. G. Sgourakis, Y. Yan, S. A. McCallum, C. Wang and A. E. Garcia, *J. Mol. Biol.*, 2007, **368**, 1448–1457.

17 C. Velez-Vega and F. A. Escobedo, *J. Phys. Chem. B*, 2011, **115**, 4900–4910.

18 D. J. Rosenman, C. R. Connors, W. Chen, C. Wang and A. E. García, *J. Mol. Biol.*, 2013, **425**, 3338–3359.

19 U. Essmann, L. Perera, M. L. Berkowitz, T. Darden, H. Lee and L. G. Pedersen, *J. Chem. Phys.*, 1995, **103**, 8577–8593.

20 B. Hess, *J. Chem. Theory. Comput.*, 2008, **4**, 116–122.

21 G. Bussi and M. Parrinello, *Computer Physics Communications*, 2008, **179**, 26–29.

22 M. Parrinello and A. Rahman, *J. Appl.Phys.*, 1981, **52**, 7182–7190.
23 O. Crescenzi, S. Tomaselli, R. Guerrini, S. Salvadori, A. M. D'Ursi, P. A. Temussi and D. Picone, *Eur. J. Biochem.*, 2002, **269**, 5642–5648.
24 Y. Sugita and Y. Okamoto, *Chem. Phys. Lett.*, 1999, **314**, 141–151.
25 A. Patriksson and D. van der Spoel, *Phys. Chem. Chem. Phys.*, 2008, **10**, 2073–2077.
26 G. Bussi, *Mol. Phys.*, 2014, **112**, 379–384.
27 W. Humphrey, A. Dalke and K. Schulten, *J. Mol. Graph.*, 1996, **14**, 33–38.
28 Y. Shen and A. Bax, *J. Biomol. NMR*, 2010, **48**, 13–22.
29 M. Karplus and D. Anderson, *J. Chem. Phys.*, 1959, **30**, 6–10.
30 B. Hess, *J. Chem. Phys.*, 2002, **116**, 209–217.
31 X. Daura, K. Gademann, B. Jaun, D. Seebach, W. F. van Gunsteren and A. E. Mark, *Angew. Chem. Int. Ed.*, 1999, **38**, 236–240.
32 W. Kabsch and C. Sander, *Biopolymers*, 1983, **22**, 2577–2637.

4 Supplementary table

Table S1 RMSD between final and initial conformer and averaged for all the 128 ABAU-MD simulations.

Segment	residues	RMSD (nm)
all	(1-42)	0.275 ± 0.111
S1	(1-16)	0.287 ± 0.141
S2	(17-21)	0.246 ± 0.095
S3	(22-29)	0.222 ± 0.090
S4	(30-42)	0.272 ± 0.142

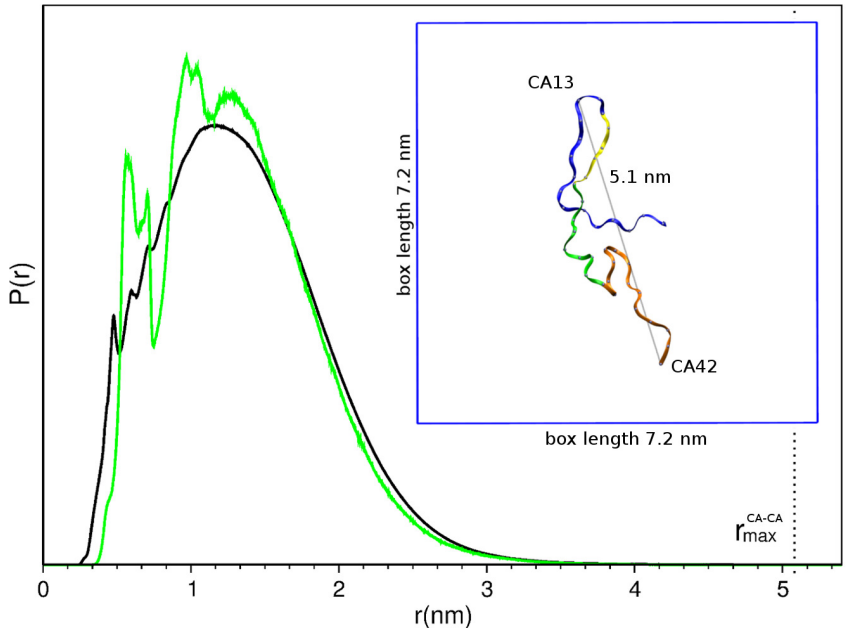

Fig. S4 Distance distribution function P(r) of Aβ42 in water (ABWT-TREMD). The black curve represents the distance distribution function of all inter-atomic distances of the heavy atoms of the peptide in water. The maximal value of r for which the distribution P(r) is non negligible (r_{max}) corresponds to the maximum diameter that Aβ42 reaches during the simulation. P(r) shows an asymmetric band with an extended tail towards high distances. The peak of the band is centered at about 0.12 nm and is due to the most populated states (i.e. the globular conformers), whereas the tail at high distances is due to the elongated states of the peptide. The green curve represents the distance distribution function of all inter-atomic distances of the C_α atoms. Peaks at small distances are due to the presence of segments arranged in secondary and tertiary structures. At distances larger than 3 nm P(r) rapidly decreases but the number of elongated conformers is not null. The inset illustrates the most extended conformation of Aβ42 in water, with a maximum C_α-C_α of 5.1 nm. The sides of the cubic box used in the simulation ABWT-TREMD are drawn explicitly.

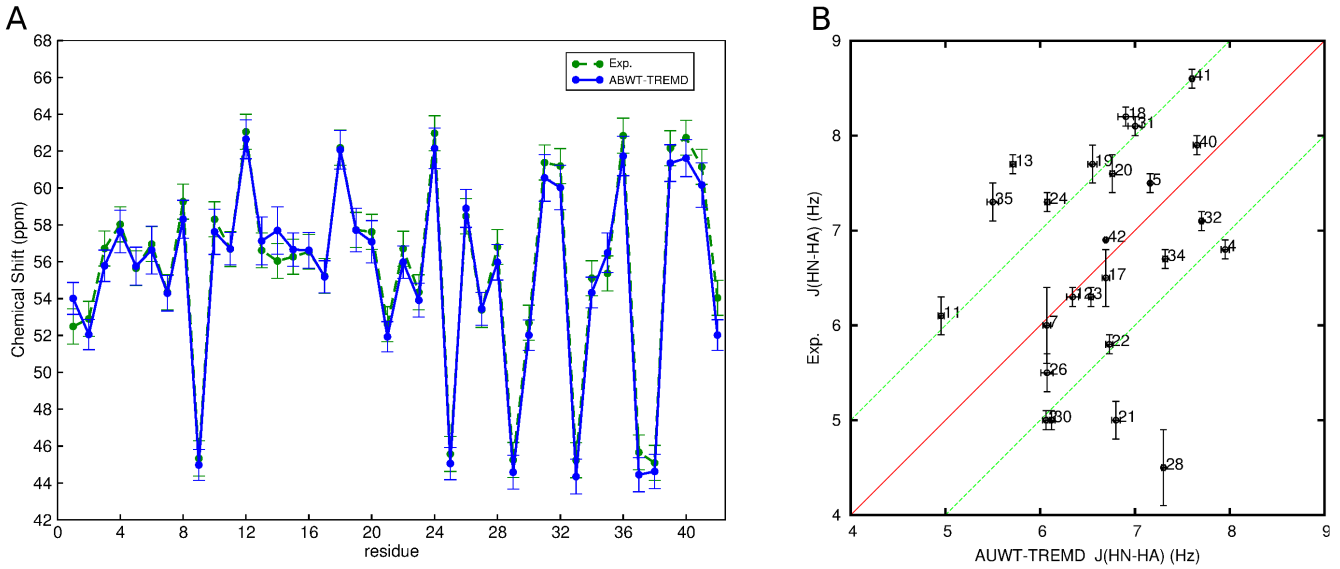

Fig. S5 Computed chemical shifts and J-couplings for ABWT-TREMD. A. Comparison between experimental data and values computed by us for ABWT-TREMD of the chemical shifts (Ref. 48 in the manuscript). The error bars for the calculated chemical shifts were obtained by SPARTA+, i.e., the σ value. B. Relation between the J-couplings J(HN-HA) calculated from simulation ABWT-REMD and the experimental values (Ref. 41 in the manuscript). The correlation between experimental and computed J(HN-NA) values is overall satisfactory, especially in view of the experimental uncertainties and of the extreme simplicity of the adopted Karplus' model for the extraction of the J values from the atomic structure.

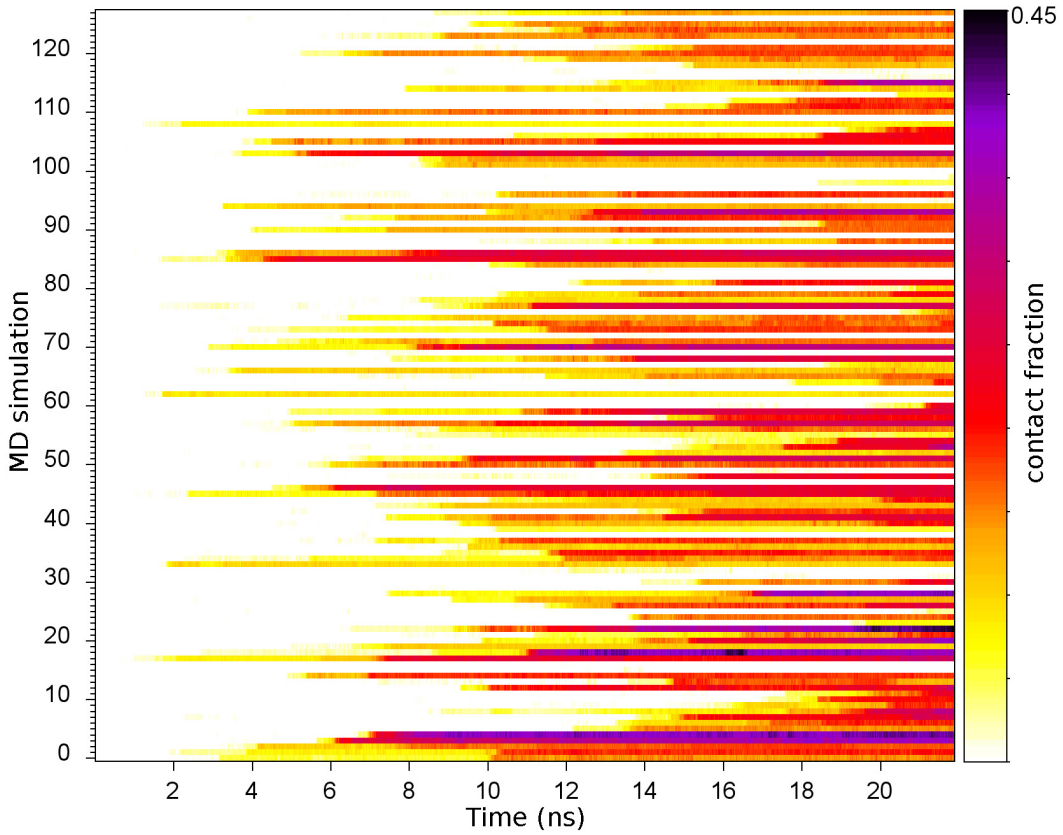

Fig. S6 Contact fraction for ABAU-MD as a function of the simulation time, for all the 128 simulations. The contact fraction is defined as the total number of contacts between the protein heavy atoms and the atoms of the gold surface, divided by the number of protein heavy atoms. We put a threshold of 0.6 nm on the establishment of a contact: namely, there is contact when the distance between an atom of the protein and a gold atom is smaller than 0.6 nm. This threshold corresponds to the situation where the peptide penetrates the water layer at the gold surface and starts to interact directly with gold.

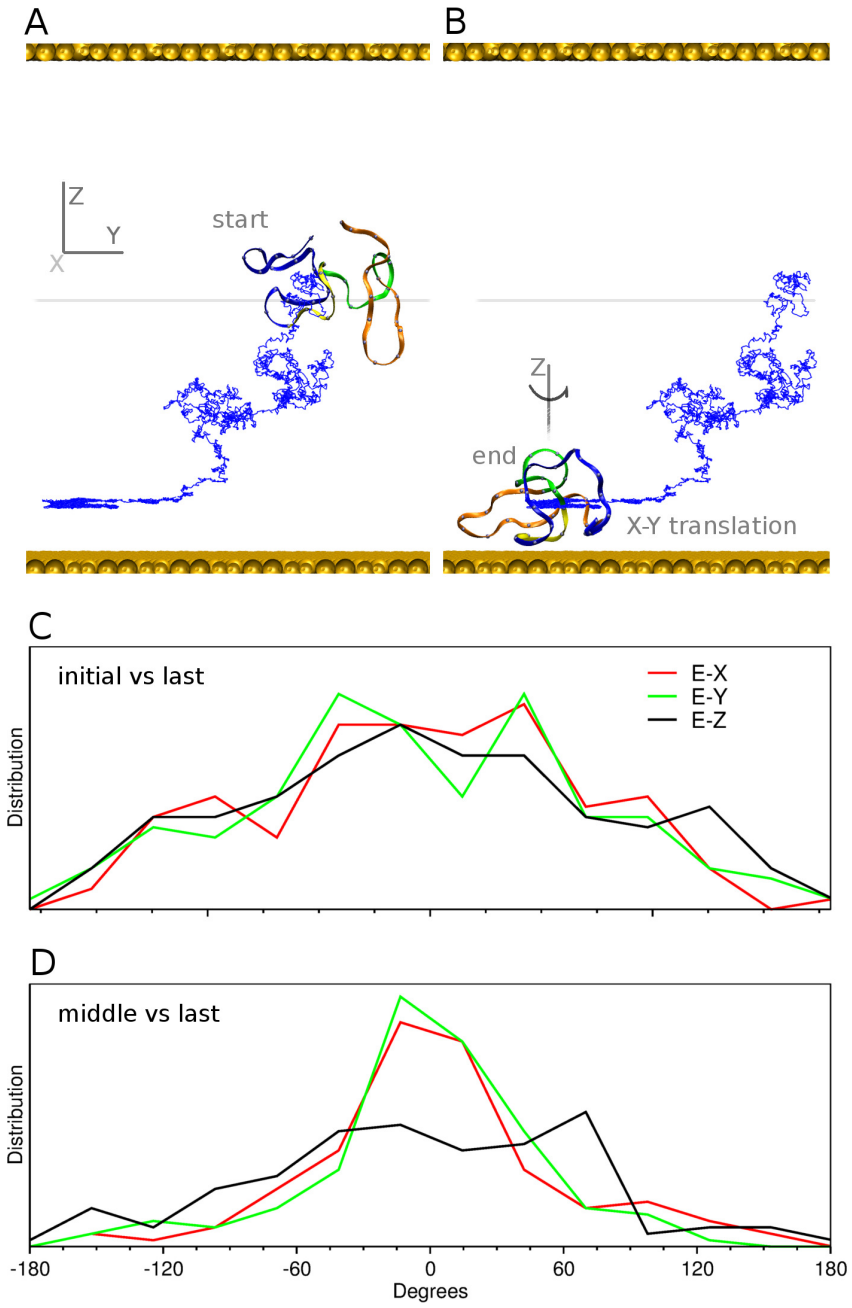

Fig. S7 Pathway and rotations of the center of mass (COM) for ABAU-MD. The COM path for ABAU-MD is illustrated as a blue trace, while the peptide is illustrated in different simulation stages (A and B) in a color code as defined in Fig. S1: yellow spheres represent gold atoms. A. At the beginning of the simulation, the peptide (centered in the simulation box) starts to diffuse and eventually adsorbs onto the gold surface. B. Peptide adsorbed onto the gold surface. In the early adsorption stages rotation along $z-$axis and translation in the $x-y$ plane are allowed. C. Distribution of Euler's angles that superimpose the final to the initial structure, averaged over all the 128 simulations. D. Distribution of Euler's angles that superimpose the final structure to the structure at 10 ns, averaged over all the 128 simulations: we see that rotation along the $z-$axis is not totally inhibited.

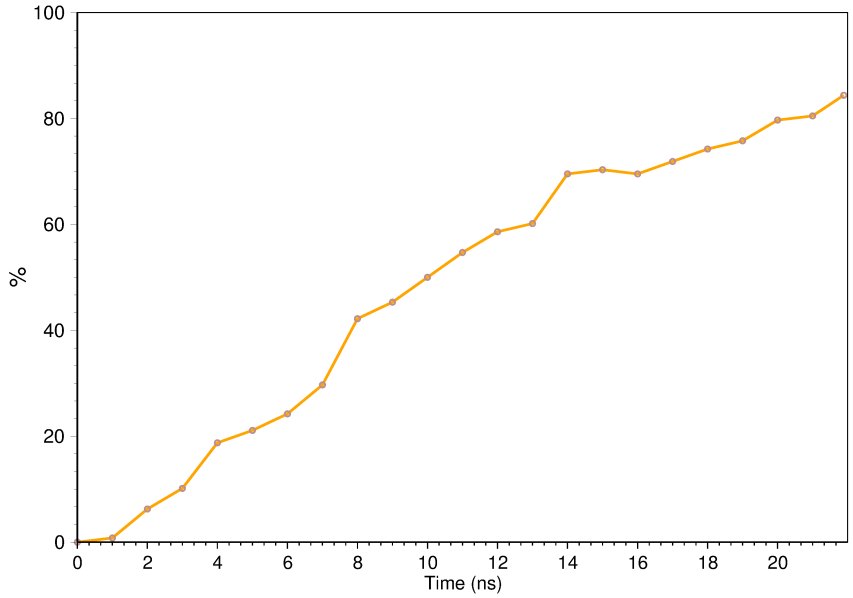

Fig. S8 Adsorption percentage of ABAU-MD. This curve was extracted from the 128 MD simulations at 300 K, i.e., ABAU-MD. A Peptide is considered adsorbed onto the gold surface if it has more than one atom at a distance smaller than 0.6 nm from the surface. At the end of the ABAU-MD simulations more than 80% of the peptides are engaged with the surface.

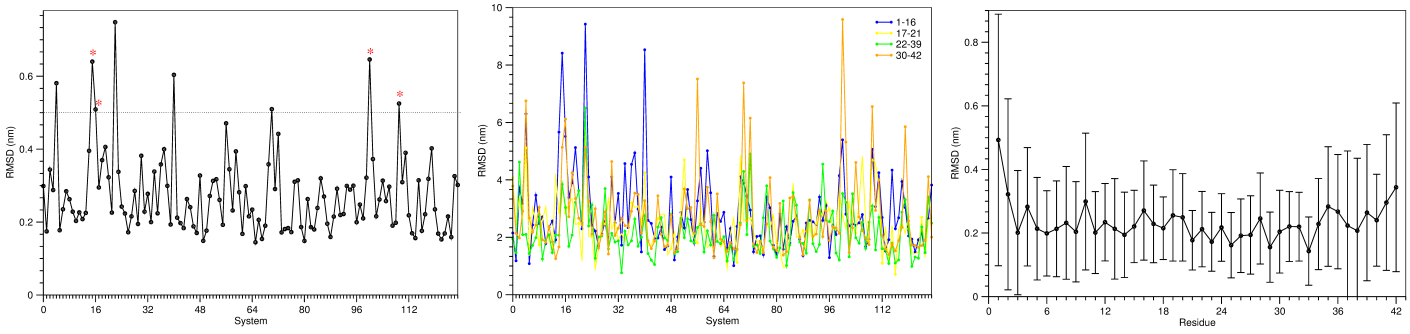

Fig. S9 RMSD of Aβ42 during the adsorption process. Left: RMSD of the 128 final structures relative to the initial structures, for ABAU-MD, including all protein atoms. There are 8 systems with RMSD larger than 0.5 nm (horizontal dashed line). Such systems undergo substantial conformational rearrangements during MD runs. Nevertheless, in 4 of the 8 systems (marked with red asterisks), Aβ42 does not interact with the gold surface. Therefore, such high deviations could equally likely be due to the conformational fluctuations of Aβ42 or to the interaction with the substrate. Thus, a high RMSD is not a strict index of peptide-gold interaction. Center: Partial RMSD of the peptide from ABAU-MD structures at 20 ns, evaluated with respect to the initial structures, considering all the atoms of the peptide. Right: Peptide RMSD resolved by residues, for ABAU-MD structures at 20 ns, evaluated with respect to the initial structures, considering all the atoms of the protein and averaged over the 128 MD simulations.

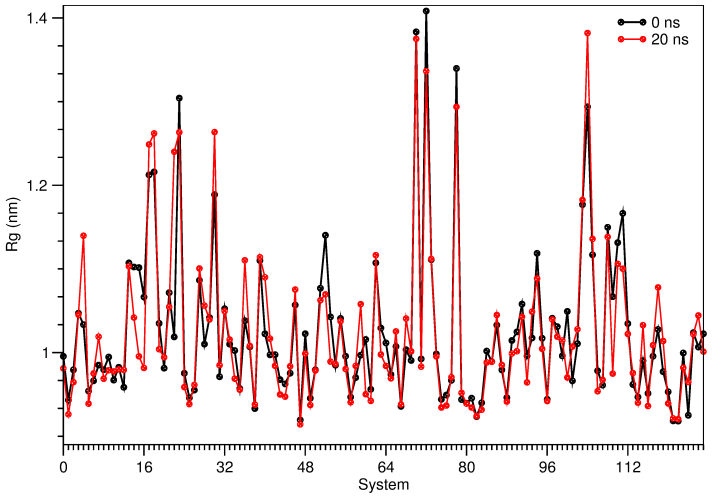

Fig. S10 Radius of Gyration for ABAU-MD. R_g evaluated (considering all the protein atoms) for the Aβ42 conformers at 0 ns (black) and at 20 ns (red). The horizontal axis runs over the 128 copies of the system.

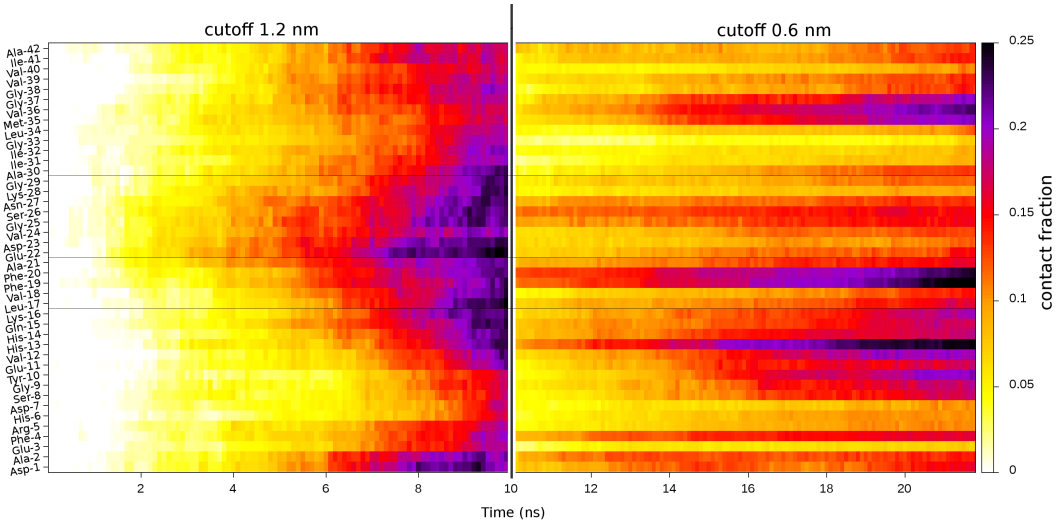

Fig. S11 Contact fraction in ABAU-MD: cutoff 1.2 nm vs 0.6 nm. Left: average contact fraction per residue (cutoff at 1.2) during the first 10 ns of simulation, indicating for each residue how many of the simulations have reached a distance of less than 1.2 nm from the surface. This fraction is not expected to be affected by the presence of the surface, and thus only depends on the geometry of the peptide. Right: average contact fraction per residue from 10 ns to the end of the simulation, indicating for each residue how many of the simulations have reached a distance of less than 0.6 nm from the surface. This fraction is affected by the presence of the surface and reflects the preferential interaction of the different residues.

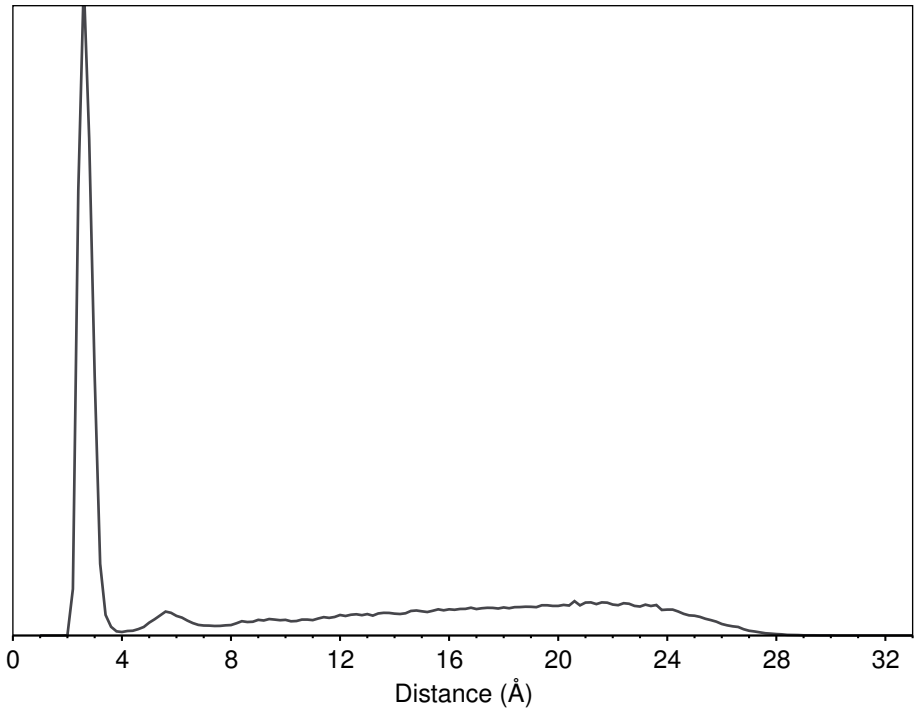

Fig. S12 Minimum distance distribution. Summary of the minimum peptide-gold distance distribution mediated over the 128 adsorption trajectories. The sharp peak at around 3Å is due to the adsorbed peptide, the peak at around 5-6Å is due to a water-mediated adsorption state that is preliminary to the anchoring on the surface, see also Fig. 3C in the main text.

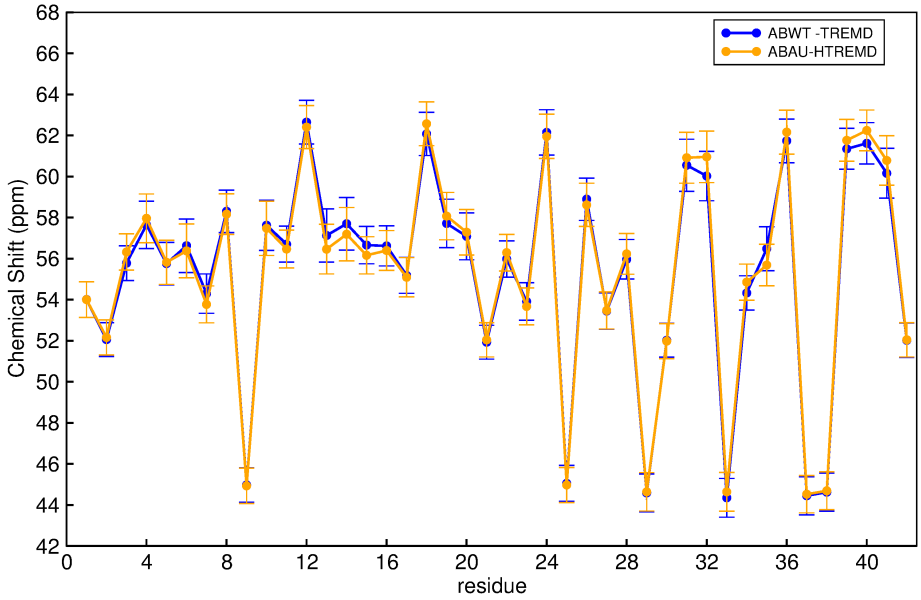

Fig. S13 Chemical Shifts. Chemical shift per residue: blue and orange curves represent ABWT-TREMD and ABAU-HTREMD, respectively. Aβ42 chemical shifts for ABAU-HTREMD are somewhat modified relative to ABWT-TREMD, to an extent that decays with the distance between the protein atom and the gold surface.

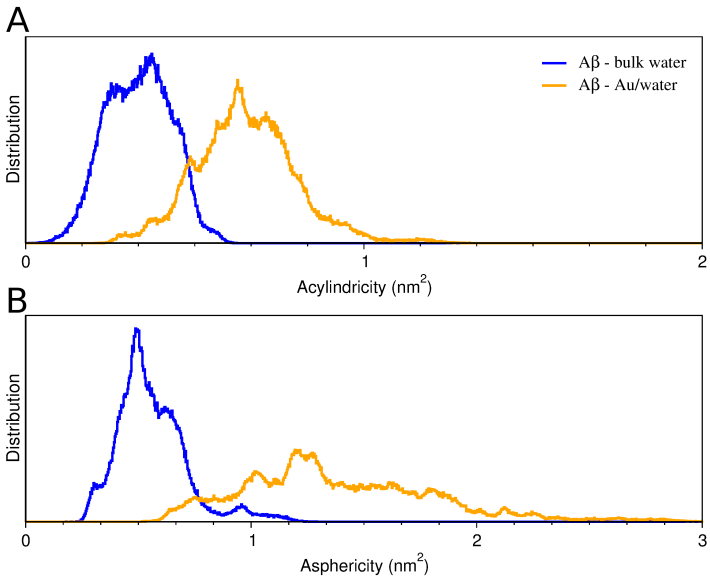

Fig. S14 Acylindricity and Asphericity. Distribution of the acylindricity (A) and asphericity (B), which are relevant quantities that characterize the shape of the peptide, for ABWT-TREMD (blue) and ABAU-HTREMD (yellow). The acylindricity measures the deviation of the protein from a cylindrical object (acylindricity equal to zero). The asphericity measures the deviation of the protein from a spherical object (asphericity equal to zero).

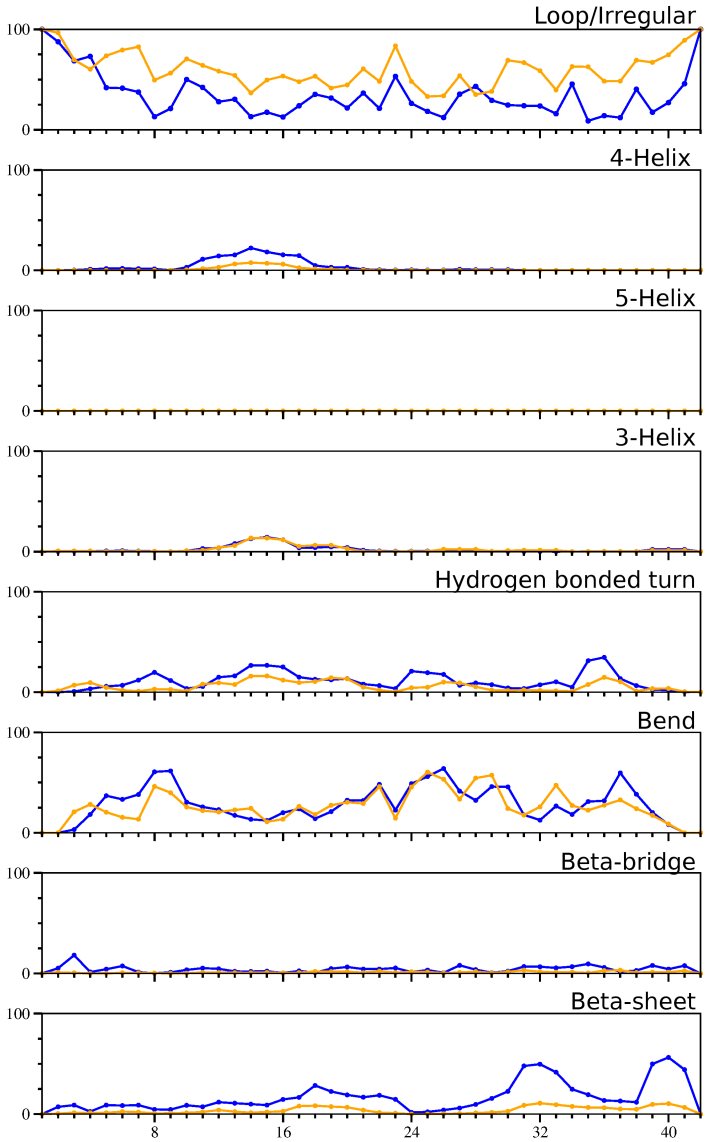

Fig. S15 **DSSP analysis.** Percentage of secondary structures: blue and orange curves represent ABWT-TREMD and ABAU-HTREMD, respectively. Definitions used in compact form in the article: HELIX (2H+3I+4G), BETA(7B+8E), BEND/TURN(5S+6T), Loop/irregular (1C).

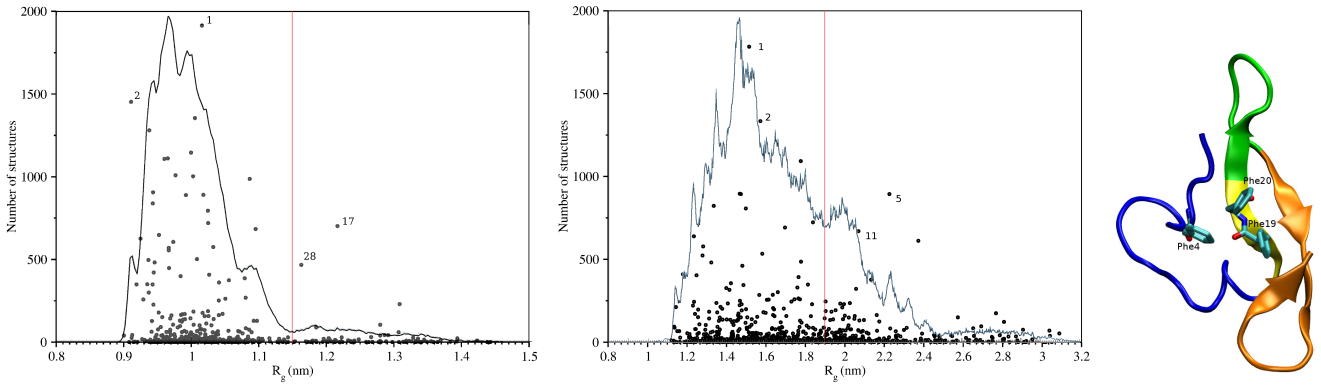

Fig. S16 Distribution of the radius of gyration over representative structures obtained from clustering. Left: Distribution (curve) of the radius of gyration of Aβ42 in solution (ABWT-TREMD): the representative structures of the 484 obtained clusters are shown as dots. The distribution shows two regions: one main peak is centered at 1 nm and a broad tail extends to R_g values larger than 1.15 nm. The peak at 1 nm is due to the globular conformers, whereas the broad region at higher values is due to extended/flat conformers, suggesting the presence of two major conformational groups, the globular and elongated states. Representative structures of clusters 1 and 2 (17 and 28), indicated in the plot with numeric labels in order of increasing cluster population, are illustrative of the globular (elongated) group and are discussed in the text. Center: Distribution (curve) of the radius of gyration of Aβ42 at the gold/water interface (ABAU-HTREMD): the representative structures of the 877 obtained clusters are shown as dots. This distribution is markedly shifted to larger R_g values and elongated structures are more abundantly populated. Representative structures of clusters 1 and 2 (5 and 11), indicated in the plot with numeric labels in order of increasing cluster population, are illustrative of less and more elongated states and are discussed in the text. Right: The most populated cluster in solution has a globular shape. Other representative structures are illustrated in Fig. 7 in the main text. Cluster 17 (Fig. 7C) is composed of the most elongated structures, whereas cluster 2 (Fig. 7B) contains the most globular states, with region S2 involved in a helix structure. Cluster 1 (Fig. 7A) and cluster 28 show (Fig. 7D) an antiparalell β-sheet motif between S2 and S4. This motif is reminiscent of the β-hairpin observed in the monomeric Aβ40 bound to the affibody $Z_{A\beta 3}$. Moreover, cluster 28 shows a peculiar β-meander motif composed of S2, A30-L36 and V39-I41 β strands. Interestingly, clusters 1 (Fig. 7A) and 28 (Fig. 7D) share a similar hairpin motif, but they differ in the arrangement of S1. In the most populated cluster, S1 interacts with S2 and S3 forming a collapsed loop in the region between Lys16 and His6, thus promoting the interaction between Phe4 and the phenil-motif, i.e., the residues Phe19 and Phe20 (Fig. S16, right). The N-terminal tail interacting with the hydrophobic core (S2) appears to shield the hairpin motif from the environment. Alternatively, in the cluster 28, S1 does not interact with S2, promoting a pronounced hairpin motif, which is quite exposed and therefore prone to interact with surrounding peptides.

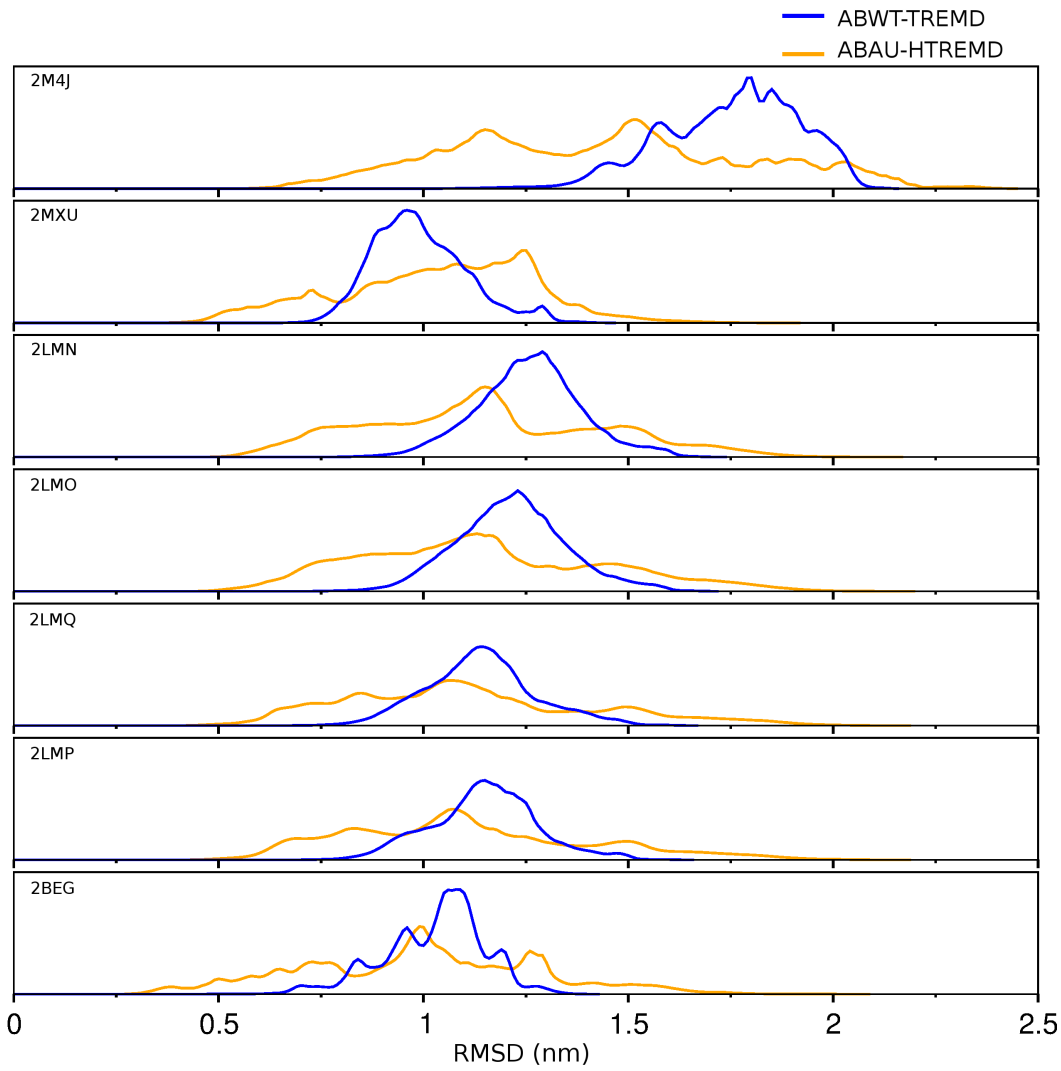

Fig. S17 Distribution of the RMSD values of ABWT-TREMD (blue) and ABAU-HTREMD (yellow) with respect to experimental fiber structures. These plots complement the data compiled in Table 1.

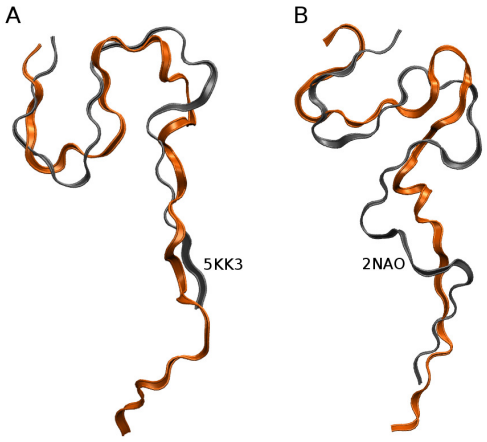

Fig. S18 ABAU-HTREMD conformations (orange) that have the lowest RMSD value with respect to the experimental structure (gray). (A) Superposition of the most similar conformation ABAU-HTREMD on the 5KK3 NMR model. (B) Superposition of the most similar conformation of the ABAU-HTREMD on 2NAO.